F. Appendix: TCE Non-Cancer Dose-Response Analyses

F.1. Data Sources

Data sources are cited in the body of this report in the section describing dose-response analyses (Section 5).

F.2. Dosimetry

This section describes some of the more detailed dosimetry calculations and adjustments used in Section 5.1.

F.2.1. Estimates of TCE in air from urinary metabolite data using Ikeda et al. (1972)

F.2.1.1. *Results for Chia et al. (1996)*

Chia et al. (1996) demonstrated a dose-related effect on hyperzoospermia in male workers exposed to TCE, lumping subjects into four groups based on range of TCA in urine.

Table F.1. Dose-response data from Chia et al. (1996)

TCA, mg per gm. creatinine	no. of subjects	no. with hyperzoospermia
0.8 to <25	37	6
50 to <75	18	8
75 to <100	8	4
>= 100 to 136.4	5	3

Minimum and maximum TCA levels are reported in the text of Chia et al. (1996), the other data, in their Table 5.

We used data from Ikeda et al. (1972) to estimate the TCE exposure concentrations corresponding to the urinary TCA levels reported by Chia et al. (1996). Ikeda et al. (1972) studied ten workshops, in each of which TCE vapour concentration was "relatively constant." They measured atmospheric concentrations of TCE and concentrations in workers' urine of total tri-chloro compounds (TTC), TCA, and creatinine, and demonstrated a linear relation between TTC/creatinine (mg/gm) in urine and TCE in the work atmosphere. Their data are tabulated as geometric means (the last column was calculated by us, as described below).

Table F.2. Data on TCE in air (ppm) and urinary metabolite concentrations in workers reported by Ikeda et al. (1972).

n	TCE (ppm)	TTC (mg/L)	TCA (mg/L)	TTC (mg/g creatinine)	TCA (mg/g creatinine)
9	3	39.4	12.7	40.8	13.15127
5	5	45.6	20.2	42.4	18.78246
6	10	60.5	17.6	47.3	13.76
4	25	164.3	77.2	122.9	57.74729
4	40	324.9	90.6	221.2	61.68273
5	45	399	138.4	337.7	117.137
5	50	418.9	146.6	275.8	96.52012
5	60	468	155.4	359	119.2064
4	120	915.3	230.1	518.9	130.4478
4	175	1210.9	235.8	1040.1	202.5399

We used these data to construct the last column "TCA.cr.mg.gm" (mg TCA/gm creatinine), as follows: TCA (mg/g creatinine) = TCA (mg/L) × TTC (mg/g creatinine) / TTC (mg/L). We then evaluated the regression relation between TCE (ppm) and TCA (mg/gm creatinine) using these data. Ikeda et al. (1972) reported that the measured values are lognormally distributed and exhibit heterogeneity of variance, and that the reported data (above) are geometric means. Thus, we used the regression relation between log10(TCA (mg/g creatinine)) and log10(TCE (ppm)), assuming constant variances and using number of subjects "n" as weights. The results are shown in Figure F.1.

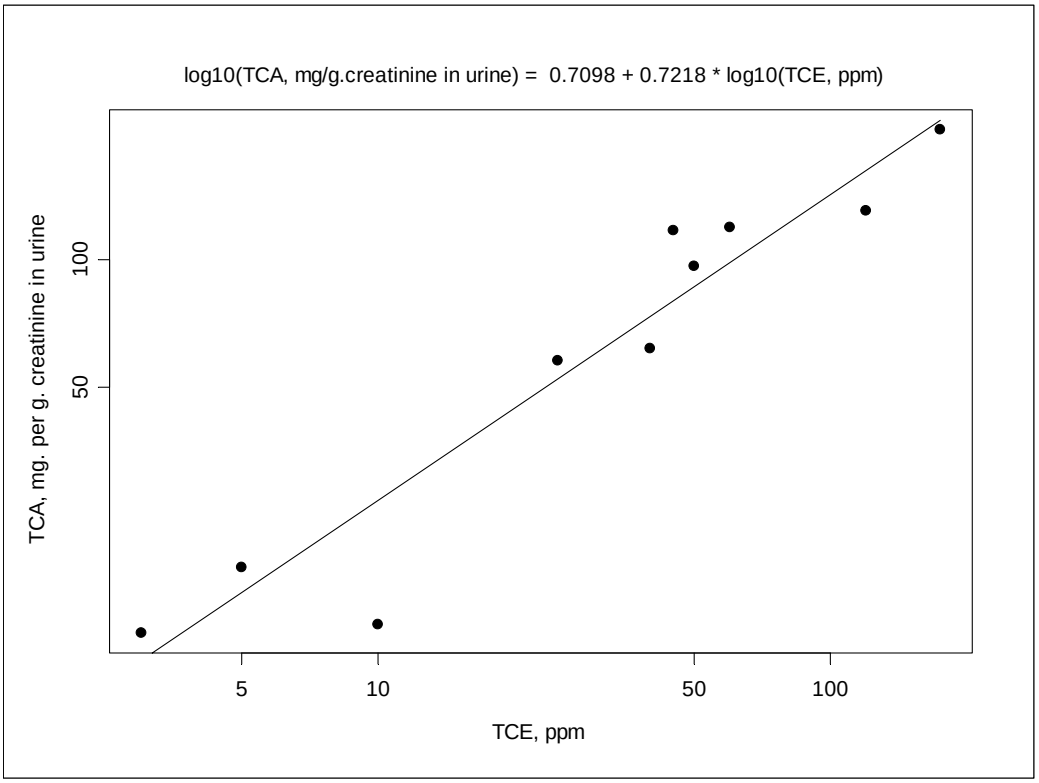


```
Coefficients:
                Value Std. Error t value Pr(>|t|)
   (Intercept) 0.7098 0.1132     6.2688  0.0002
log10(TCE.ppm) 0.7218 0.0771     9.3578  0.0000

Residual standard error: 0.3206 on 8 degrees of freedom
Multiple R-Squared: 0.9163
F-statistic: 87.57 on 1 and 8 degrees of freedom, the p-value is
0.0000139
```

Figure F.1. Regression of TCE in air (ppm) and TCA in urine (mg/g creatinine) based on data from Ikeda et al. (1972).

Next, we assumed a Berkson setting for linear calibration, in which we wanted to predict X (TCE, ppm) from means for Y (TCA, mg/gm creatinine), with substantial error in Y (Snedecor and Cochran, 1980). Thus we used inverse prediction for the data of Chia et al. (1996) to infer their mean TCE exposures. The relation based on data from Ikeda et al. (1972) is

```
log10(TCA, mg/g.creatinine)  =   0.7098 + 0.7218*log10(TCE, ppm)
```

and the inverse prediction is

```
log10(TCE) = (log10(TCA) - 0.7098)/0.7218
TCE, ppm   = 10^( (log10(TCA) - 0.7098)/0.7218 )
```

Because of the lognormality of data reported by Ikeda et al. (1972), we used the means of the logarithms of the ranges for TCA (mg/gm creatinine) in Chia et al. (1996), which is an estimate of the median for the group. The results are shown in Table F.3.

Table F.3. Estimated urinary metabolite and TCE air concentrations in dose groups from Chia et al. (1996)

TCA, mg per gm. Creatinine	Estim. TCA median [a]	log10(TCA median)	Estim. ppm TCE [b]
0.8 to <25	4.47	0.650515	0.827685
50 to <75	61.2	1.787016	31.074370
75 to <100	86.6	1.937531	50.226119
>= 100 to 136.4	117	2.067407	76.008668

[a] 10^(mean(log10(TCA limits in first column)))

[b] 10^((log10(TCA median)) - 0.7098)/0.7218

We modeled dose-response relations for the data of Chia et al. (1996) using both the estimated medians for TCA (mg/gm creatinine) in urine and estimated TCE (ppm in air) as doses. The TCE - TCA - TTC relations are linear up to about 75 ppm TCE (Figure 1 of Ikeda et al. 1972), and certainly in the range of the BMD. As noted below (Section F.2.2), the occupational exposure levels are further adjusted to equivalent continuous exposure for deriving the point of departure (POD).

F.2.1.2. *Results for Mhiri et al. (2004)*

The LOAEL group for abnormal trigeminal nerve somatosensory evoked potential reported in Mhiri et al. (2004) had a urinary TCA concentration of 32.6 mg TCA/mg creatinine. Using the above "inverse prediction" equation gives an occupational exposure level = 10^((log10(32.6) – 0.7098)/0.7218) = 12.97404 ppm. As noted below (Section F.2.2), the occupational exposure levels are further adjusted to equivalent continuous exposure for deriving the point of departure (POD).

F.2.2. Dose Adjustments to applied doses for intermittent exposure

The nominal applied dose was adjusted for exposure discontinuity (e.g., exposure for 5 days per week and 6 hours per day reduced the dose by the factor (5/7)*(6/24)). The PBPK dose metrics took into account the daily and weekly discontinuity to produce an equivalent average

dose for continuous exposure. No dose adjustments were made for duration of exposure or a less-than-lifetime study, as is typically done for cancer risk estimates, though in deriving the candidate reference values, an Uncertainty Factor for subchronic-to-chronic exposure was applied where appropriate.

For human occupational studies, inhalation exposures (air concentrations) were adjusted by the number of work (versus non-work) days and the amount of air intake during working hours as a fraction of the entire day (10 m^3 during work/20 m^3 for entire day). For the TCE ppm in air converted from urinary metabolite data using Ikeda et al. (1972), the work week was 6 days, so the adjustment for number of work days is 6/7.

F.2.3. PBPK model-based internal dose metrics

PBPK modeling was used to estimate levels of dose metrics corresponding to different exposure scenarios in rodents and humans (Section 3.5). The selection of dose metrics for specific organs and endpoints is discussed under Section 5.1.

The PBPK model requires an average body weight. For most of the studies, we used averages specific to each species, strain, and sex. Where these were not reported in the text of an article, data were obtained by digitizing the body weight graphics (Maltoni et al., 1986) or by finding the median of weekly averages from graphs (NCI 1976; NTP, 1990, 1988). Where necessary, we used default adult body weights specific to the strain (USEPA, 1994).

F.3. Dose-Response Modeling Procedures

Where adequate dose-response data were available, we fitted models with the BMDS software (http://www.epa.gov/ncea/bmds) using the applicable applied doses or PBPK model-based dose metrics for each combination of study, species, strain, sex, endpoints, and BMR under consideration.

F.3.1. Models for dichotomous response data

F.3.1.1. *Quantal models*

For dichotomous responses, we fitted the loglogistic, multistage, and Weibull models. These models adequately describe the dose-response relationship for the great majority of datasets, specifically in past TCE studies (Filipsson and Victorin, 2003). If the slope parameter of the loglogistic model was less than 1, indicating a supralinear dose-response shape, we also fitted the model with the slope constrained to 1 for comparison. For the multistage model, we used an order one less than the number of dose groups, in addition to the 2^{nd}-order multistage

model if it differed from the preceding model, and the first-order ('linear') multistage model (which is identical to a Weibull model with power parameter equal to 1). We also fitted the Weibull model with the power parameter unconstrained.

F.3.1.2. *Nested dichotomous models*

In addition, nested dichotomous models were used for developmental effects in rodent studies to account for possible litter effects, such maternal covariates or intra-litter correlation. The available nested models in BMDS are the nested loglogistic model, the Rai-VanRyzin Models, and the NCTR model. Candidates for litter-specific covariates (LSC) were identified from the studies and considered legitimate for analysis if they were not significantly dose-related (determined via regression, analysis of variance). The need for a LSC was indicated by a difference of at least 3 in the AIC for models with and without a LSC. The need to estimate intra-litter correlations (IC) was determined by presence of a high correlation coefficient for at least one dose group and by AIC. The fits for nested models were also compared with the results from quantal models.

F.3.2. Models for continuous response data

For continuous responses, we fitted the distinct models available in BMDS: power model (power parameter unconstrained and constrained to ≥ 1), polynomial model, and Hill model. Both constant variance and modeled variance models were fit; but constant variance models were used for model parsimony unless the p-value for the test of homogenous variance was <0.10, in which case the modeled variance models were considered. For the polynomial model, model order was selected as follows. A model of order 1 was fitted first. The next higher order model (up to order n-1) was accepted if AIC decreased more than 3 units and the p-value for the mean did not decrease.

F.3.3. Model selection

After fitting these models to the datasets, we applied the recommendations for model selection set out in EPA's Benchmark Dose Technical Guidance Document (Inter-Agency Review Draft, US EPA, 2008b). First, models were generally rejected if the p-value for goodness of fit was < 0.10. In a few cases in which none of the models fit the data with $p>0.10$, linear models were selected on the basis of an adequate visual fit overall. Second, models were rejected if they did not appear to adequately fit the low-dose region of the dose-response relationship, based on an examination of graphical displays of the data and scaled residuals. If the BMDL estimates from the remaining models were "sufficiently close" (we used a criterion of

within 2-fold for "sufficiently close"), then the model with the lowest Akaike Information Criteria (AIC) was selected. The AIC is a measure of information loss from a dose-response model that can be used to compare a set of models. Among a specified set of models, the model with the lowest AIC is considered the "best". If 2 or more models share the lowest AIC, the BMD Technical Guidance Document (US EPA, 2008b) suggests that an average of the BMDLs could be used, but averaging was not used in this assessment (for the one occasion in which models shared the lowest AIC, a selection was made based on visual fit). If the BMDL estimates from the remaining models are not sufficiently close, some model dependence is assumed. With no clear biological or statistical basis to choose among them, the lowest BMDL was chosen as a reasonable conservative estimate, as suggested in the Benchmark Dose Technical Guidance Document, unless the lowest BMDL appeared to be an outlier, in which case further judgments were made.

F.3.4. Additional adjustments for selected datasets

In a few cases, the dose-response data necessitated further adjustments in order to improve model fits.

The behavioral/neurological endpoint "number of rears" from Moser et al. (1995) consisted of counts, measured at five doses and four measurement times (with 8 observations each). The high dose for this endpoint was dropped because the mean was zero, and no monotone model could fit that well. Analysis of means and standard deviations for these counts suggested a Box-Cox power transform (Box et al., 1978) of ½ (i.e., square root) to stabilize variances (i.e., the slope of the regression of log(SD) on log(mean) was 0.46, and the relation was linear and highly significant). This information was helpful in selecting a suitable variance model with high confidence (i.e., variance constant, for square-root transformed data). Thus, the square root was taken of the original individual count data, and the mean and variance of the transformed count data were used in the BMD modeling.

The high dose group was dropped due to supra-linear dose-response shapes in two cases: fetal cardiac malformations from Johnson et al. (2003) and decreased PFC response from Woolhiser et al. (2006). Johnson et al. (2003) is discussed in more detail below (Section F.4.2.1). For Woolhiser et al. (2006), model fit near the BMD and the lower doses as well as the model fit to the variance were improved by dropping the highest dose (a procedure suggested in U.S. EPA (2008b).

In some cases, the supralinear dose-response shape could not be accommodated by these measures, and a LOAEL or NOAEL was used instead. These include NCI (1976) (toxic nephrosis, >90% response at lowest dose), Keil et al. (2009) (autoimmune markers and decreased

thymus weight, only two dose groups in addition to controls), and Peden-Adams et al. (2006) (developmental immunotoxicity, only two dose groups in addition to controls).

F.4. Dose-Response Modeling Results

F.4.1. Quantal dichotomous and continuous modeling results

The documents Appendix.linked.files\AppF.Non-cancer.Plots.TCE.contin.DRAFT.pdf and Appendix.linked.files\AppF.Non-cancer.Plots.TCE.dichot.DRAFT.pdf show the fitted model curves. The graphics include observations (group means or proportions), the estimated model curve (solid red line) and estimated BMD, with a BMDL. Vertical bars show 95% confidence intervals for the observed means. Printed above each plot are some key statistics (necessarily rounded) for model goodness of fit and estimated parameters. Printed in the plots in the upper left are the BMD and BMDL for the rodent data, in the same units as the rodent dose.

More detailed results, including alternative BMRs, alternative dose metrics, quantal analyses for endpoints for which nested analyses were performed, etc. are documented in the several spreadsheets. Input data for the analyses are in the following documents: Appendix.linked.files\AppF.Non-cancer.Input.Data.TCE.contin.DRAFT.pdf and Appendix.linked.files\AppF.Non-cancer.Input.Data.TCE.dichot.DRAFT.pdf. The documents Appendix.linked.files\AppF.Non-cancer.Results.TCE.contin.DRAFT.pdf and Appendix.linked.files\AppF.Non-cancer.Results.TCE.dichot.DRAFT.pdf present the data and model summary statistics, including goodness-of-fit measures (Chi-square goodness-of-fit P-value, AIC), parameter estimates, BMD, and BMDL. The group numbers "GRP" are arbitrary and are the same as GRP numbers in the plots. Note finally that not all plots are shown in the documents above, since these spreadsheets include many "alternative" analyses.

F.4.2. Nested dichotomous modeling results

F.4.2.1. *Johnson et al. (2003) fetal cardiac defects*

F.4.2.1.1. *Results using applied dose*

The biological endpoint was frequency of rat fetuses having cardiac defects, as shown in Table F.4. Individual animal data were kindly provided by Dr. Johnson (personal communication from Paula Johnson, University of Arizona, to Susan Makris, U.S. EPA, 26 August 2009). Cochran-Armitage trend tests using number of fetuses and number of litters indicated significant increases in response with dose (with or without including the highest dose).

Table F.4. Data on fetuses and litters with abnormal hearts from Johnson et al. (2003)

Dose group (mg/kg/day):	0	0.00045	0.048	0.218	129
FETUSES					
Number of pups:	606	144	110	181	105
Abnormal Heart:	13	0	5	9	11
LITTERS					
Number of litters:	55	12	9	13	9
Abnormal Heart:	9	0	4	5	6

One suitable candidate for a LSC was available: female weight gain during pregnancy. Based on goodness of fit, this covariate did not contribute to better fit and was not used. Some ICs were significant and these parameters were included in the model.

With the high dose included, the chi-square goodness of fit was acceptable, but some residuals were large (1.5 to 2) for the control and two lower doses. Therefore, models were also fitted after dropping the highest dose. For these, goodness of fit was adequate and scaled residuals were smaller for the low doses and control. Predicted expected response values were closer to observed when the high dose was dropped, as shown in Table F.5:

Table F.5. Comparison of observed and predicted numbers of fetuses with abnormal hearts from Johnson et al. (2003), with and without the high dose group, using a nested model.

	Abnormal Hearts (pups)				
Dose group (mg/kg/day):	0	0.00045	0.048	0.218	129
Observed:	13	0	5	9	11
Predicted expected:					
with high dose	19.3	4.5	3.5	5.7	11
without high dose	13.9	3.3	3.4	10	--

Accuracy in the low-dose range is especially important because the BMD is based upon the predicted responses at the control and the lower doses. Based on the foregoing measures of goodness of fit, we used the model based on dropping the high dose.

The Nested LogLogistic and Rai-VanRyzin models were fitted; these gave essentially the same predicted responses and POD. The former model was used as the basis for a POD; results are in Table F.6 and Figure F.2.

Table F.6. Results of nested loglogistic model for fetal cardiac anomalies from Johnson et al. (2003) without the high dose group, on the basis of applied dose (mg/kg/d in drinking water)

model	LSC?	IC?	AIC	Pval	BMR	BMD	BMDL
NLOG	Y	Y	246.877	NA (df=0)	0.01	0.252433	0.03776
NLOG	Y	N	251.203	0.0112	0.01	0.238776	0.039285
NLOG	N	N	248.853	0.0098	0.01	0.057807	0.028977
NLOG	N	Y	243.815	0.0128	0.1	0.71114	0.227675
NLOG	N	Y	243.815	0.0128	0.05	0.336856	0.107846
NLOG*	N	**Y**	**243.815**	**0.0128**	**0.01**	**0.064649**	**0.020698**

NLOG = "nested loglogistic" model

LSC analyzed was female weight gain during pregnancy.

* Indicates model selected (Rai-VanRyzin model fits are essentially the same)

Figure F.2. BMD modeling of Johnson et al. (2003) using nested loglogistic model, with applied dose, without LSC, with IC, and without the high dose group, using a BMR of 0.05 extra risk (top panel) or 0.01 extra risk (bottom panel).

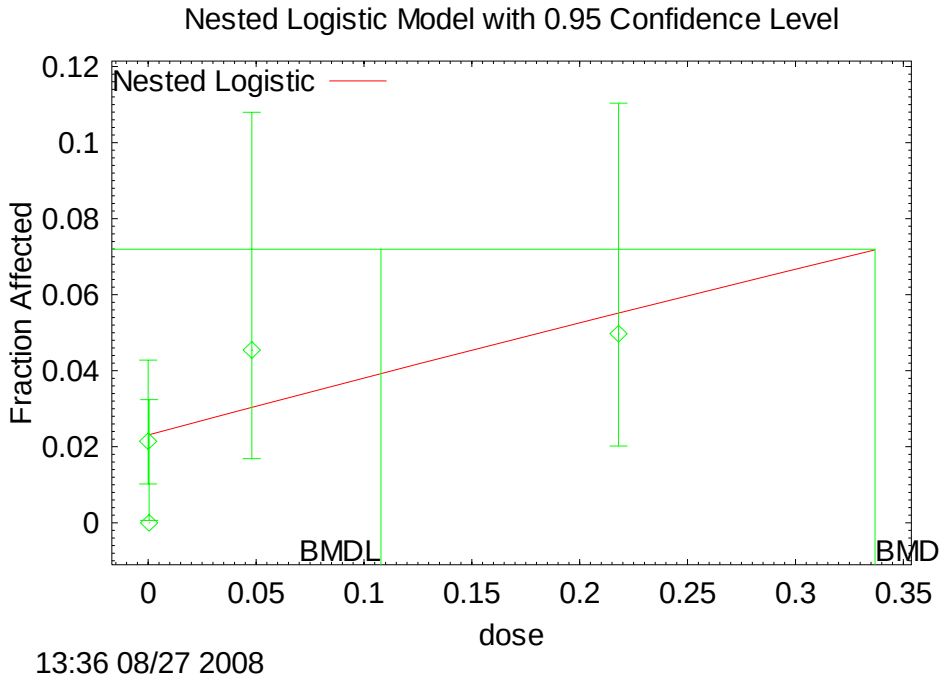

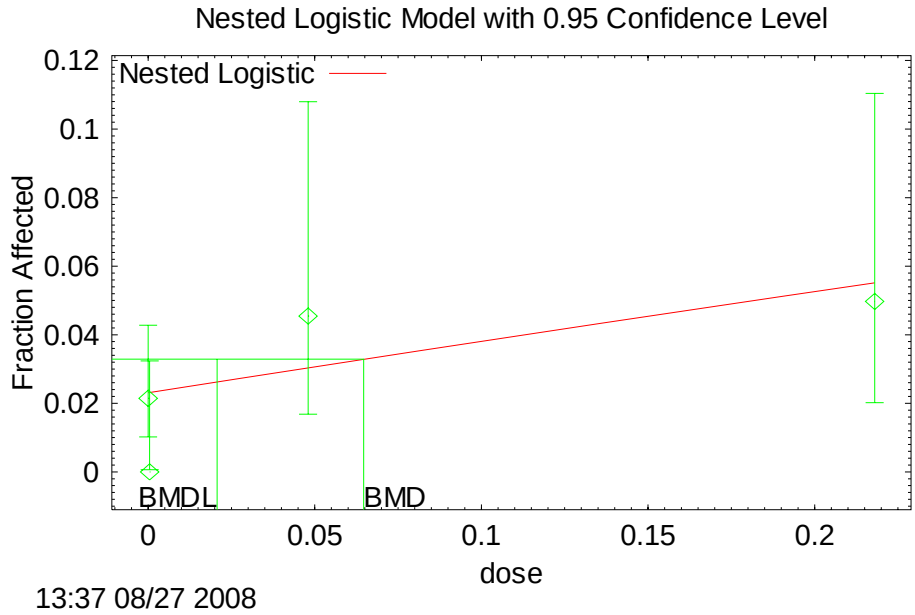

F.4.2.1.2. *Chi-square Goodness of Fit Test for Nested Loglogistic*

The BMDS choice of subgroups did not seem appropriate given the data. The high dose group of 13 litters was subdivided into three subgroups having sums of expected counts 3, 3, and 2. However, the control group of 55 litters could have been subdivided because expected response rates for controls were relatively high. We were also concerned that the goodness of fit might change with alternative choices of subgroupings.

An R program was written to read the BMDS output, reading parameters and the table of litter-specific results (dose, covariate, estimated probability of response, litter size, expected response count, observed response count, scaled chi-square residual). The control group of 55 litters was subdivided into three subgroups of 18, 18, and 19 litters. Control litters were sampled randomly without replacement 100 times, each time creating 3 subgroups - i.e., 100 random assignments of the 55 control litters to three subgroups were made. For each of these, the goodness-of-fit calculation was made and the p-value saved. Within these 100 p-values, ≥75% were ≥0.05, and ≥50% had p-values ≥0.11, this indicated that the model is acceptable based on goodness-of-fit criteria.

F.4.2.1.3. *Results using PBPK model-based dose metrics*

The nested loglogistic model was also run using the dose metrics in the dams of total oxidative metabolism scaled by body weight to the ¾-power (TotOxMetabBW34) and the area-under-the-curve of TCE in blood (AUCCBld). As with the applied dose modeling, LSC (maternal weight gain) was not included, but IC was included, based on the criteria outlined previously (Section F.3.1.2). The results are summarized in Table F.7 and Figure F.3 for TotOxMetabBW34 and Table F.8 and Figure F.4 for AUCCBld.

Table F.7. Results of nested loglogistic model for fetal cardiac anomalies from Johnson et al. (2003) without the high dose group, using the TotOxMetabBW34 dose metric

model	LSC?	IC?	AIC	Pval	BMR	BMD	BMDL
NLOG	Y	Y	246.877	NA (df=0)	0.01	0.174253	0.0259884
NLOG	Y	N	251.203	0.0112	0.01	0.164902	0.0270378
NLOG	N	Y	243.815	0.0128	0.1	0.489442	0.156698
NLOG*	**N**	**Y**	**243.815**	**0.0128**	**0.01**	**0.0444948**	**0.0142453**
NLOG	N	N	248.853	0.0098	0.01	0.0397876	0.0199438

NLOG = "nested loglogistic" model

LSC analyzed was female weight gain during pregnancy.

* Indicates model selected. BMDS failed with the Rai-VanRyzin and NCTR models.

Figure F.3. BMD modeling of Johnson et al. (2003) using nested loglogistic model, with TotOxMetabBW34 dose metric, without LSC, with IC, and without the high dose group, using a BMR of 0.01 extra risk.

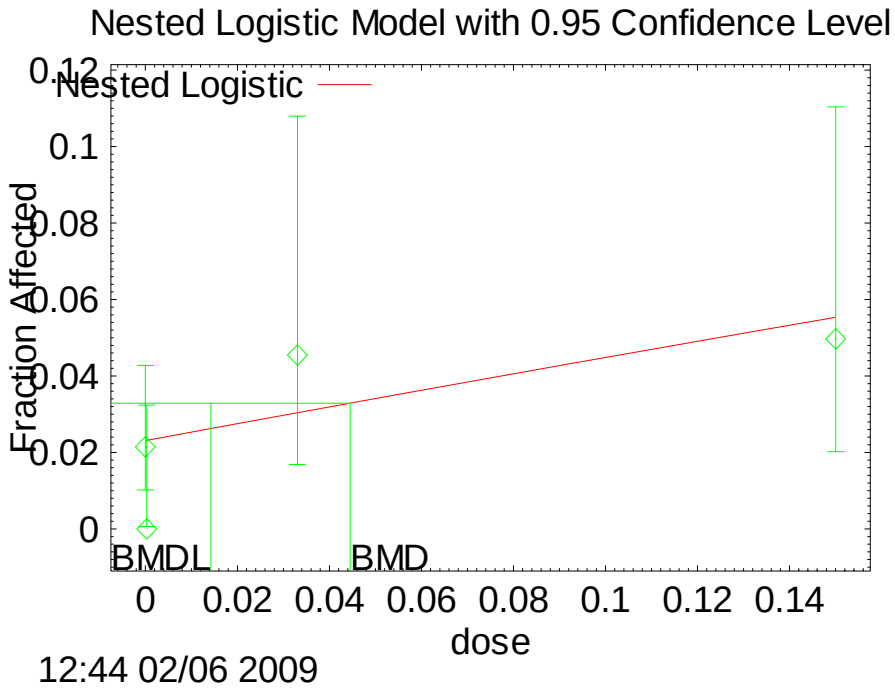

Table F.8. Results of nested loglogistic model for fetal cardiac anomalies from Johnson et al. (2003) without the high dose group, using the AUCCBld dose metric

model	LSC?	IC?	AIC	Pval	BMR	BMD	BMDL
NLOG	Y	Y	246.877	NA (df=0)	0.01	0.00793783	0.00118286
NLOG	Y	N	251.203	0.0112	0.01	0.00750874	0.00123047
NLOG*	N	Y	243.816	0.0128	0.1	0.0222789	0.00712997
NLOG*	**N**	**Y**	**243.816**	**0.0128**	**0.01**	**0.00202535**	**0.000648179**
NLOG	N	N	248.853	0.0098	0.01	0.00181058	0.000907513

NLOG = "nested loglogistic" model

LSC analyzed was female weight gain during pregnancy.

* Indicates model selected. BMDS failed with the Rai-VanRyzin and NCTR models.

Figure F.4. BMD modeling of Johnson et al. (2003) using nested loglogistic model, with AUCCBld dose metric, without LSC, with IC, and without the high dose group, using a BMR of 0.01 extra risk.

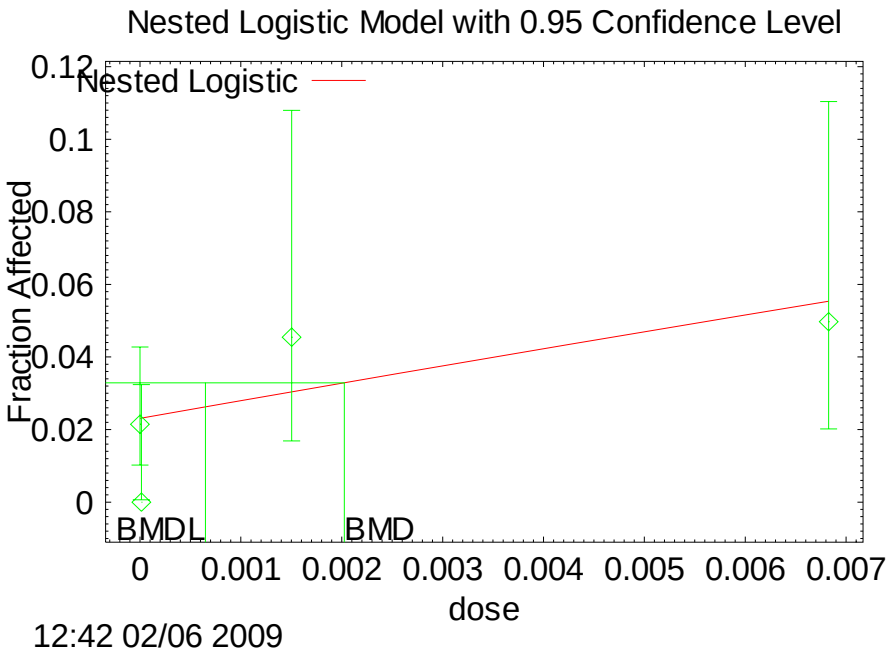

F.4.2.2. *Narotsky et al. (1995)*

Data were combined for the high doses in the single-agent experiment and the lower doses in the 'five-cube' experiment. Individual animal data were kindly provided by Dr. Narotsky (personal communications from Michael Narotsky, U.S. EPA, to John Fox, U.S. EPA, 19 June 2008, and to Jennifer Jinot, U.S. EPA, 10 June 2008). Two endpoints were examined: frequency of eye defects in rat pups and prenatal loss (number of implantation sites minus number of live pups on postnatal day 1).

Two LSCs were considered, with analyses summarized in Table F.9. The number of implants is unrelated to dose, as inferred from regression and analysis of variance, and was considered as a LSC for eye defects. As number of implants is part of the definition for the endpoint of prenatal loss, it is not considered as a LSC for prenatal loss. A second LSC, the dam body weight on GD6 (damBW6) was significantly related to dose and is unsuitable as a litter-specific covariate.

Table F.9. Analysis of LSCs with respect to dose from Narotsky et al. (1995)

Relation of litter-specific covariates to dose			
Implants:	none		
damBW6:	significant		
	TCE	Mean Implants	Mean damBW6
	0	9.5	176.0
	10.1	10.1	180.9
	32	9.1	174.9
	101	7.8	170.1
	320	10.4	174.5
	475	9.7	182.4
	633	9.6	185.3
	844	8.9	182.9
	1125	9.6	184.2
using expt as covariate, e.g.: damBW6 ~ TCE.mg.kgd + expt			
linear regression:		P=0.7486	P=0.0069
AoV (ordered factor):		P=0.1782	P=0.0927

F.4.2.2.1. *Fetal eye defects*

The Nested LogLogistic and Rai-VanRyzin models were fitted to the number of pups with eye defects reported by Narotsky et al. (1995), with the results summarized in Table F.10.

Table F.10. Results of nested loglogistic and Rai-VanRyzin model for fetal eye defects from Nartosky et al. (1995), on the basis of applied dose (mg/kg/d in drinking water).

Model	LSC?	IC?	AIC	Pval	BMR	BMD	BMDL
NLOG	Y	Y	255.771	0.3489	0.05	875.347	737.328 **
NLOG	Y	N	259.024	0.0445	0.05	830.511	661.629
NLOG	N	Y	270.407	0.2281	0.05	622.342	206.460
NLOG	N	N	262.784	0.0529	0.10	691.93	542.101
NLOG	N	N	262.784	0.0529	0.05	427.389	264.386
NLOG	N	N	262.784	0.0529	0.01	147.41	38.7117 *
RAI	Y	Y	274.339	0.1047	0.05	619.849	309.925
RAI	Y	N	264.899	0.0577	0.05	404.788	354.961
RAI	N	Y	270.339	0.2309	0.05	619.882	309.941
RAI	N	N	262.481	0.0619	0.10	693.04	346.52
RAI	N	N	262.481	0.0619	0.05	429.686	214.843
RAI	N	N	262.481	0.0619	0.01	145.563	130.938 *

NLOG = "nested loglogistic" model; RAI = Rai-VanRyzin model
LSC analyzed was implants.
* Indicates model selected.
** Graphical fit at the origin exceeds observed control and low dose responses and slope is quite flat (Figure F.5), fitted curve does not represent the data well

Results for Nested Loglogistic model suggested a better model fit with the inclusion of the LSC and IC, based on AIC. However, the graphical fit (Figure F.5) is strongly sublinear and high at the origin where the fitted response exceeds the observed low-dose responses for the control group and two low-dose groups. We selected an alternative Nested Loglogistic model without either LSC or IC (Figure F.6), which fits the low-dose responses better. Given that this model had no LSC and no IC, the nested loglogistic model reduces to a quantal loglogistic model. Parameter estimates and the p-values were essentially the same for the two models (Table F.11). A similar model selection can be justified for the Rai-Van Ryzin model. Because no LSC and no IC were needed (Figure F.12), we modeled this endpoint using quantal models, using totals of implants and losses for each dose group, which allowed choice from a wider range of models (those results appear with quantal model results in this appendix).

Figure F.5. BMD modeling of fetal eye defects from Narotsky et al. (1995) using nested loglogistic model, with applied dose, with both LSC and IC, using a BMR of 0.05 extra risk.

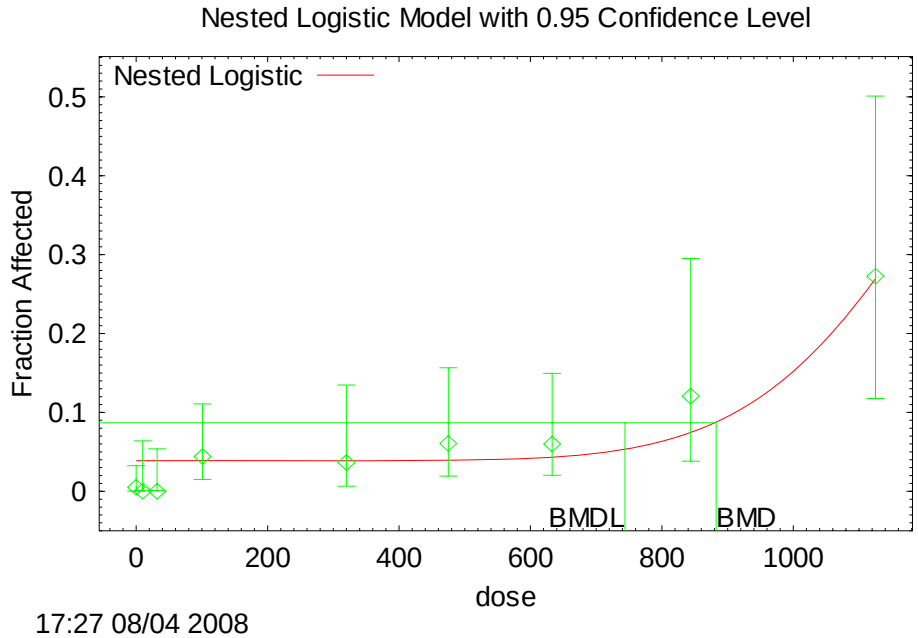

Figure F.6. BMD modeling of fetal eye defects from Narotsky et al. (1995) using nested loglogistic model, with applied dose, without either LSC or IC, using a BMR of 0.05 extra risk.

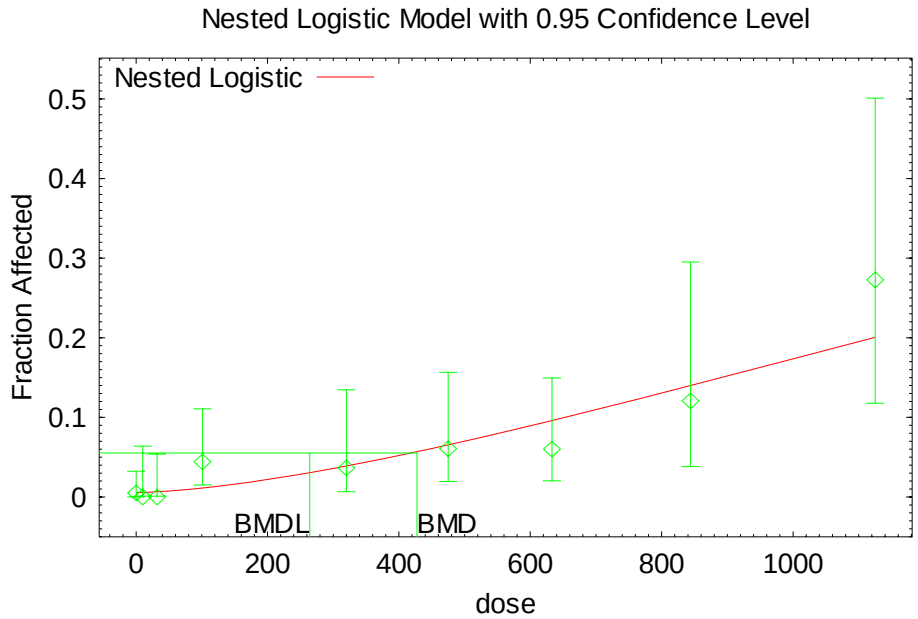

Table F.11. Comparison of results of nested loglogistic (without LSC or IC) and quantal loglogistic model for fetal eye defects from Nartosky et al. (1995).

	Parameter			BMD_{05}	$BMDL_{05}$
Model	Alpha	Beta	Rho		
Nested	0.00550062	-12.3392	1.55088	427.4	264.4
Quantal	0.00549976	-12.3386	1.55079	427.4	260.2

Figure F.7. BMD modeling of fetal eye defects from Narotsky et al. (1995) using nested Rai-VanRyzin model model, with applied dose, without either LSC or IC, using a BMR of 0.05 extra risk.

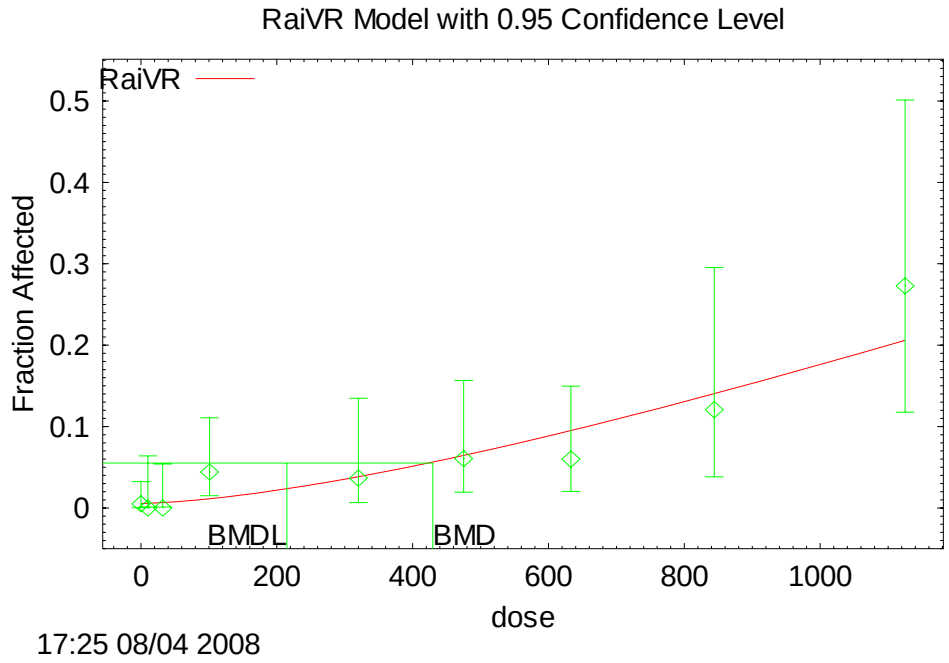

F.4.2.2.2. *Narotsky et al. (1995) prenatal loss*

The Nested LogLogistic and Rai-VanRyzin models were fitted to prenatal loss reported by Narotsky et al. (1995), with the results summarized in Table F.12.

Table F.12. Results of nested loglogistic and Rai-VanRyzin model for prenatal loss from Nartosky et al. (1995), on the basis of applied dose (mg/kg/d in drinking water).

Model	LSC?	IC?	AIC	Pval	BMR	BMD	BMDL
NLOG	Y	Y	494.489	0.2314	0.10	799.723	539.094
NLOG	Y	N	627.341	0.0000	0.10	790.96	694.673
NLOG	N	N	628.158	0.0000	0.10	812.92	725.928
NLOG	N	Y	490.766	0.2509	0.10	814.781	572.057
NLOG	N	Y	490.766	0.2509	0.05	738.749	447.077
NLOG	**N**	**Y**	**490.766**	**0.2509**	**0.01**	**594.995**	**252.437 ***
RAI	Y	Y	491.859	0.3044	0.10	802.871	669.059
RAI	Y	N	626.776	0.0000	0.10	819.972	683.31
RAI	N	N	626.456	0.0000	0.10	814.98	424.469
RAI	N	Y	488.856	0.2983	0.10	814.048	678.373
RAI	N	Y	488.856	0.2983	0.05	726.882	605.735
RAI	**N**	**Y**	**488.856**	**0.2983**	**0.01**	**562.455**	**468.713** *

NLOG = "nested loglogistic" model; RAI = Rai-VanRyzin model
LSC analyzed was dam body weight on GD6.
* Indicates model selected.

The BMDS nested models require a LSC, so we used dam body weight on GD6 ("damBW6") as the LSC. However, damBW6 is significantly related to dose and, so, is not a reliable LSC. Number of implants could not be used as a LSC because it was identified as number at risk in the BMDS models. These issues were obviated because the model selected did not employ the LSC.

For the nested loglogistic models, the AIC is much larger when the IC is dropped, so the IC is needed in the model. The LSC can be dropped (and is also suspect because it is correlated with dose). The model with IC and without LSC was selected on the basis of AIC (shown in Figure F.8). For the Rai-VanRyzin models, the model selection was similar to that for the nested loglogistic, leading to a model with IC and without LSC, which had the lowest AIC (shown in Figure F.9).

Figure F.8. BMD modeling of prenatal loss reported in Narotsky et al. (1995) using nested loglogistic model, with applied dose, without LSC, with IC, using a BMR of 0.05 extra risk (top panel) or 0.01 extra risk (bottom panel).

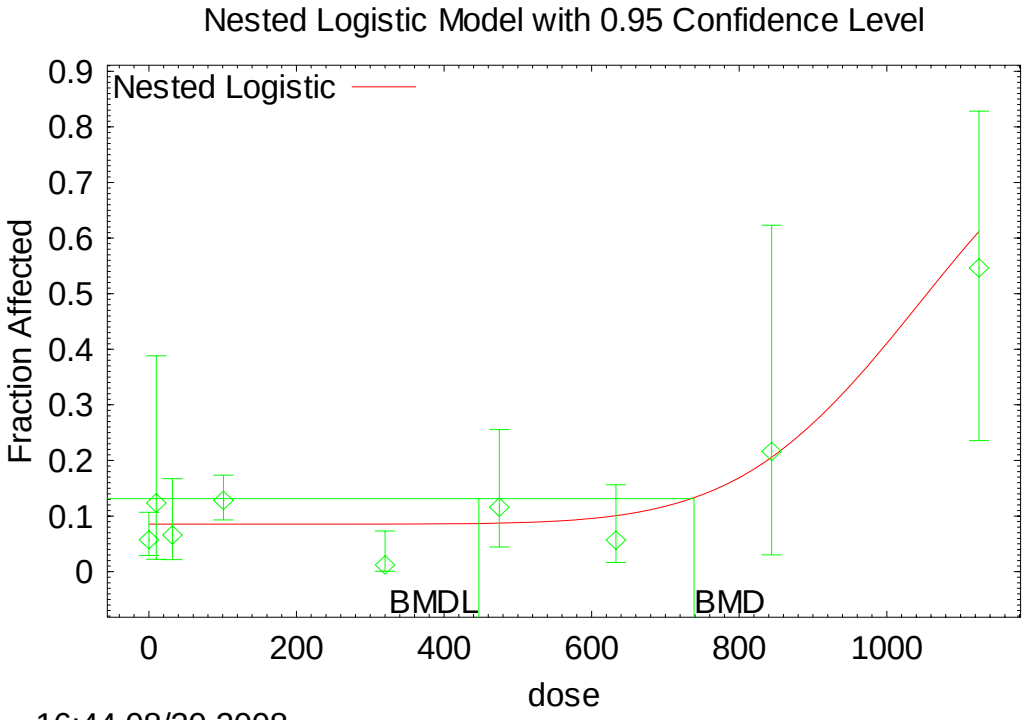

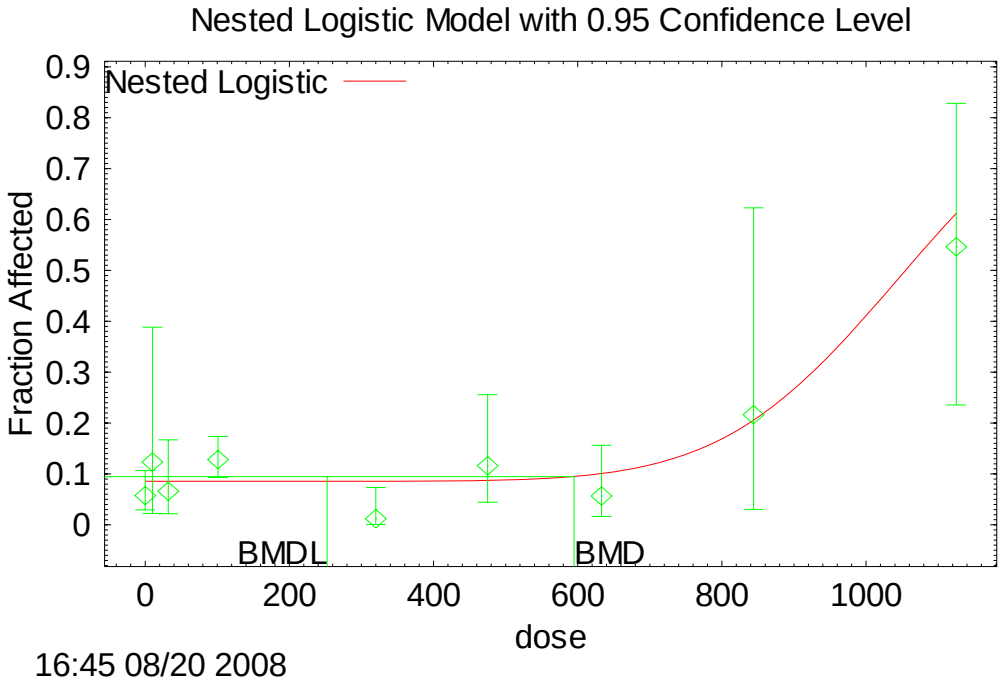

Figure F.9. BMD modeling of prenatal loss reported in Narotsky et al. (1995) using nested Rai-VanRyzin model, with applied dose, without LSC, with IC, using a BMR of 0.05 extra risk (top panel) or 0.01 extra risk (bottom panel).

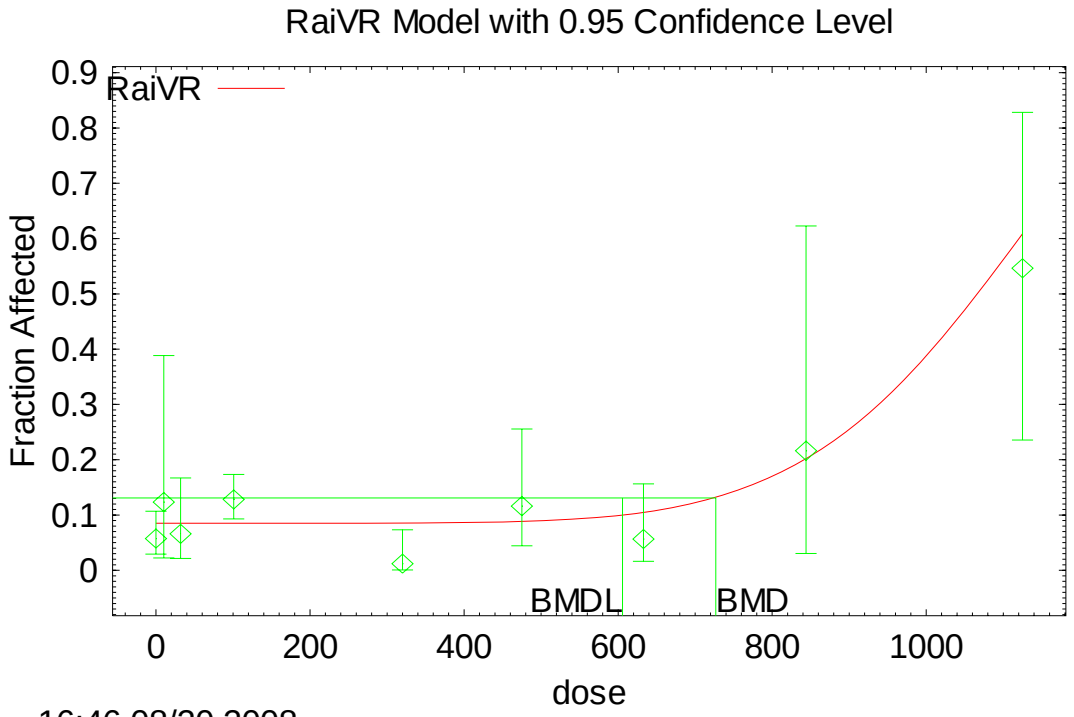

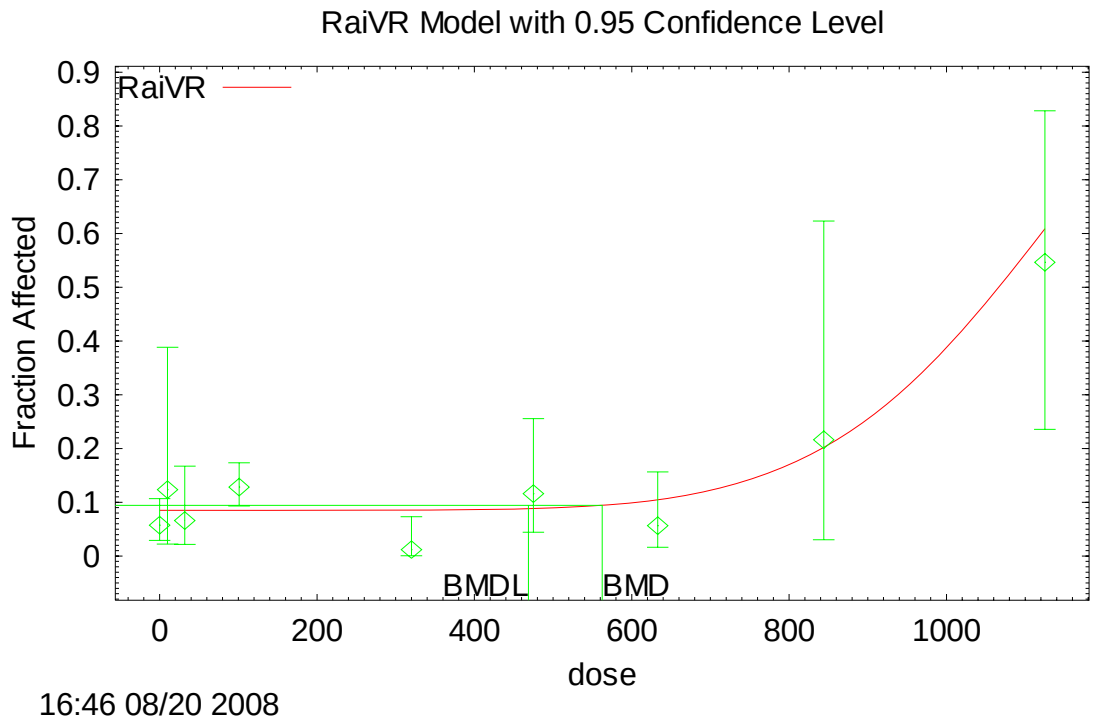

F.4.3. Model selections and results

The final model selections and results for non-cancer dose-response modeling are presented in Table F.13.

Table F.13. Model selections and results for non-cancer dose-response analyses.

GRP	Study	Species	Sex	Strain	Exposure route	Endpoint	dose metric	BMR type	BMR	BMD/ BMDL	BMDL	model	reporting BMD	Notes
Dichotomous models														
3	Chia.etal.1996	human	M	workers.elec.factory	inhal	N.hyperzoospermia	appl.dose	extra	0.1	2.14	1.43	loglogistic.1	3.06	
7	Narotsky.etal.1995	rat	F	F344	oral.gav	N.pups.eye.defects	appl.dose	extra	0.01	1.46	60.1	multistage	806	a
13	Narotsky.etal.1995.sa	rat	F	F344	oral.gav	N.dams.w.resorbed.litters	appl.dose	extra	0.01	5.47	32.2	multistage.2	570	
13	Narotsky.etal.1995.sa	rat	F	F344	oral.gav	N.dams.w.resorbed.litters	AUCCBld	extra	0.01	5.77	17.5	multistage.2	327	
13	Narotsky.etal.1995.sa	rat	F	F344	oral.gav	N.dams.w.resorbed.litters	TotMetabBW34	extra	0.01	1.77	77.5	weibull	156	
14	Johnson.etal.2003.drophi	rat	F	Sprague.Dawley	oral.dw	N.litters.abnormal.hearts	appl.dose	extra	0.1	2.78	0.0146	loglogistic.1	0.0406	b
36	Griffin etal.2000	mice	F	MRL++	oral.dw	portal.infiltration	appl.dose	extra	0.1	2.67	13.4	loglogistic.1	35.8	
38	Maltoni.etal.1986	rat	M	Sprague.Dawley	inhal	megalonucleocytosis	appl.dose	extra	0.1	1.22	40.2	multistage	49.2	c
38	Maltoni.etal.1986	rat	M	Sprague.Dawley	inhal	megalonucleocytosis	ABioactDCVCBW34	extra	0.1	1.18	0.0888	loglogistic	0.105	
38	Maltoni.etal.1986	rat	M	Sprague.Dawley	inhal	megalonucleocytosis	AMetGSHBW34	extra	0.1	1.19	0.086	loglogistic	0.102	
38	Maltoni.etal.1986	rat	M	Sprague.Dawley	inhal	megalonucleocytosis	TotMetabBW34	extra	0.1	1.13	53.8	weibull	61	d
39	Maltoni.etal.1986	rat	M	Sprague.Dawley	oral.gav	megalonucleocytosis	appl.dose	extra	0.1	1.53	33.8	multistage.2	51.8	e
49	NTP.1988	rat	F	Marshall	oral.gav	toxic nephropathy	appl.dose	extra	0.05	1.45	9.45	loglogistic.1	28.9	
49	NTP.1988	rat	F	Marshall	oral.gav	toxic nephropathy	ABioactDCVCBW34	extra	0.05	1.45	0.0132	loglogistic.1	0.0404	
49	NTP.1988	rat	F	Marshall	oral.gav	toxic nephropathy	AMetGSHBW34	extra	0.05	1.46	0.0129	loglogistic.1	0.0397	
49	NTP.1988	rat	F	Marshall	oral.gav	toxic nephropathy	TotMetabBW34	extra	0.05	1.45	2.13	loglogistic.1	6.5	
Nested dichotomous models														
NA	Johnson.etal.2003.drophi	rat	F	Sprague.Dawley	oral.dw	N.pups.abnormal.hearts	appl.dose	extra	0.01	3.12	0.0207	loglogistic.IC	0.711	b
NA	Johnson.etal.2003.drophi	rat	F	Sprague.Dawley	oral.dw	N.pups.abnormal.hearts	TotOxMetabBW34	extra	0.01	3.12	0.0142	loglogistic.IC		b
NA	Johnson.etal.2003.drophi	rat	F	Sprague.Dawley	oral.dw	N.pups.abnormal.hearts	AUCCBld	extra	0.01	3.12	0.000648	loglogistic.IC		b
NA	Narotsky.etal.1995	rat	F	F344	oral.gav	N.prenatal.loss	appl.dose	extra	0.01	1.2	469	RAI.IC	814	
Continuous models														
2	Land.etal.1981	mouse	M	(C57B1xC3H)F1	inhal	pct.abnormal.sperm	appl.dose	standard	0.5	1.33	46.9	polynomial.constvar	125	
6	Carney.etal.2006	rat	F	Sprague-Dawley (Crl:CD)	inhal	gm.wgt.gain.GD6.9	appl.dose	relative	0.1	2.5	10.5	hill	62.3	
8	Narotsky.etal.1995	rat	F	F344	oral.gav	gm.wgt.gain.GD6.20	appl.dose	relative	0.1	1.11	108	polynomial.constvar	312	
19	Crofton.etal.97	rat	M	Long-Evans	inhal	dB.auditory.threshold(16kHz)	appl.dose	absolute	10	1.11	274	polynomial.constvar	330	
21	George.etal.1986	rat	F	F344	oral.food	litters	appl.dose	standard	0.5	1.69	179	polynomial.constvar	604	
23	George.etal.1986	rat	F	F344	oral.food	live.pups	appl.dose	standard	0.5	1.55	152	polynomial.constvar	470	
26	George.etal.1986	rat	F	F344	oral.food	Foffspring.BWgm.day21	appl.dose	relative	0.05	1.41	79.7	polynomial.constvar	225	
34sq	Moser.etal.1995+perscom	rat	F	F344	oral.gav	no.rears	appl.dose	standard	1	1.64	248	polynomial.constvar	406	b,f
49	George.etal.1986	rat	F	F344	oral.food	traverse.time.21do	appl.dose	relative	1	1.98	72.6	power	84.9	
51	Buben.O'Flaherty.85	mouse	M	SwissCox	oral.gav	Liverwt.pctBW	appl.dose	relative	0.1	1.26	81.5	hill.constvar	92.8	
51	Buben.O'Flaherty.85	mouse	M	SwissCox	oral.gav	Liverwt.pctBW	AMetLiv1BW34	relative	0.1	1.08	28.6	polynomial.constvar	28.4	
51	Buben.O'Flaherty.85	mouse	M	SwissCox	oral.gav	Liverwt.pctBW	TotOxMetabBW34	relative	0.1	1.08	37	polynomial.constvar	36.7	
58	Kjellstrand.etal.1983b	mouse	M	NMRI	inhal	Liverwt.pctBW	appl.dose	relative	0.1	1.36	21.6	hill	30.4	
58	Kjellstrand.etal.1983b	mouse	M	NMRI	inhal	Liverwt.pctBW	AMetLiv1BW34	relative	0.1	1.4	22.7	hill	32.9	
58	Kjellstrand.etal.1983b	mouse	M	NMRI	inhal	Liverwt.pctBW	TotOxMetabBW34	relative	0.1	1.3	73.4	hill	97.7	
60.Rp	Kjellstrand.etal.1983b	mouse	M	NMRI	inhal	Kidneywt.pctBW	appl.dose	relative	0.1	1.17	34.7	polynomial	47.1	
60.Rp	Kjellstrand.etal.1983b	mouse	M	NMRI	inhal	Kidneywt.pctBW	AMetGSHBW34	relative	0.1	1.18	0.17	polynomial	0.236	
60.Rp	Kjellstrand.etal.1983b	mouse	M	NMRI	inhal	Kidneywt.pctBW	TotMetabBW34	relative	0.1	1.17	71	polynomial	95.2	
63	Woolhiser.etal.2006	rat	F	CD (Sprague-Dawley)	inhal	Antibody.Forming Cells	appl.dose	standard	1	1.94	31.2	power.constvar	60.6	b
62	Woolhiser.etal.2006	rat	F	CD (Sprague-Dawley)	inhal	Antibody.Forming Cells	AUCCBld	standard	1	1.44	149	polynomial	214	
62	Woolhiser.etal.2006	rat	F	CD (Sprague-Dawley)	inhal	Antibody.Forming Cells	TotMetabBW34	standard	1	1.5	40.8	polynomial	61.3	
65	Woolhiser.etal.2006	rat	F	CD (Sprague-Dawley)	inhal	kidney.wt.per100gm	appl.dose	relative	0.1	4.29	15.7	hill.constvar	54.3	
65	Woolhiser.etal.2006	rat	F	CD (Sprague-Dawley)	inhal	kidney.wt.per100gm	ABioactDCVCBW34	relative	0.1	4.27	0.0309	hill.constvar	0.103	
65	Woolhiser.etal.2006	rat	F	CD (Sprague-Dawley)	inhal	kidney.wt.per100gm	AMetGSHBW34	relative	0.1	4.28	0.032	hill.constvar	0.107	
65	Woolhiser.etal.2006	rat	F	CD (Sprague-Dawley)	inhal	kidney.wt.per100gm	TotMetabBW34	relative	0.1	1.47	40.8	polynomial.constvar	52.3	
67	Woolhiser.etal.2006	rat	F	CD (Sprague-Dawley)	inhal	liver.wt.per100gm	appl.dose	relative	0.1	4.13	25.2	hill.constvar	70.3	
67	Woolhiser.etal.2006	rat	F	CD (Sprague-Dawley)	inhal	liver.wt.per100gm	AMetLiv1BW34	relative	0.1	1.53	46	polynomial.constvar	56.1	
67	Woolhiser.etal.2006	rat	F	CD (Sprague-Dawley)	inhal	liver.wt.per100gm	TotOxMetabBW34	relative	0.1	1.53	48.9	polynomial.constvar	59.8	

Applied dose BMDLs are in units of ppm in air for inhalation exposures and mg/kg/d for oral exposures. Internal dose BMDLs are in dose metric units. Reporting BMD is BMD using a BMR of 0.1 extra risk for dichotomous models, and 1 control SD for continuous models.
loglogistic = unconstrained loglogistic; loglogistic.1 = constrained loglogistic; multistage = multistage with #stages=dose groups-1; multistage.n = n-stage multistage; loglogistic.IC = nested loglogistic with IC, without LSC; RAI.IC = Rai-VanRyzin model with IC, without LSC
zzz.constvar = continuous model zzz with constant variance (otherwise variance is modeled)

Notes:

a Eight-stage multistage model.
b Dropped highest dose.
c Three-stage multistage model.
d Weibull selected over loglogistic w/same AIC on basis of visual fit (less extreme curvature).
e Second-order MS selected on basis of visual fit (less extreme curvature).
f Square-root transformation of original individual count data.

F.5. Derivation of points of departure

F.5.1. Applied dose points of departure

For oral studies in rodents, the point of departure (POD) on the basis of applied dose in mg/kg/d was taken to be the BMDL, NOAEL, or LOAEL. NOAELs and LOAELs were adjusted for intermittent exposure to their equivalent continuous average daily exposure (for BMDLs, the adjustments were already performed prior to BMD modeling).

For inhalation studies in rodents, the POD on the basis of applied dose in ppm was taken to be the BMDL, NOAEL, or LOAEL. NOAELs and LOAELs were adjusted for intermittent exposure to their equivalent continuous average daily exposure (for BMDLs, the adjustments were already performed prior to BMD modeling). These adjusted concentrations are considered human equivalent concentrations, in accordance with U.S. EPA (1994), as TCE is considered a Category 3 gas (systemically acting) and has a blood-air partition coefficient in rodents greater than that in humans (see Section 3.1).

F.5.2. PBPK model-based human points of departure

As discussed in Section 5.1.3, the PBPK model was used for simultaneous inter-species (for endpoints in rodent studies), intra-species, and route-to-route extrapolation (rtr) based on the estimates from the PBPK model of the internal dose points of departure (iPOD) for each candidate critical study/endpoints. The following documents contain figures showing the derivation of the human equivalent doses and concentrations (HEDs and HECs) for the median (50^{th} percentile) and sensitive (99^{th} percentile) individual from the (rodent or human) study iPOD. In each case, for a specific study/endpoint(s)/sex/species (in the figure main title), and for a particular dose metric (y-axis label), the horizontal line shows the original study iPOD (a BMDL, NOAEL, or LOAEL as noted) and where it intersects with the human 99^{th} percentile (open square) or median (closed square) exposure-internal-dose relationship:

Appendix.linked.files\AppF.Non-cancer.HECs.Plots.human.inhalation.studies.TCE.DRAFT.pdf
Appendix.linked.files\AppF.Non-cancer.HECs.Plots.rodent.inhalation.studies.TCE.DRAFT.pdf
Appendix.linked.files\AppF.Non-cancer.HECs.Plots.rodent.oral.studies.TCE.DRAFT.pdf
Appendix.linked.files\AppF.Non-cancer.HEDs.Plots.human.inhalation.studies.TCE.DRAFT.pdf
Appendix.linked.files\AppF.Non-cancer.HEDs.Plots.rodent.inhalation.studies.TCE.DRAFT.pdf
Appendix.linked.files\AppF.Non-cancer.HEDs.Plots.rodent.oral.studies.TCE.DRAFT.pdf

The original study internal doses are based on the median estimates from about 2000 "study groups" (for rodent studies) or "individuals" (for human studies), and corresponding exposures for the human median and 99th percentiles were derived from a distribution of 2000 "individuals." In both cases, the distributions reflect combined uncertainty (in the population means and variances) and population variability.

In addition, as part of the uncertainty/variability analysis described in Section 5.1.4.2, the POD for studies/endpoints for which BMD modeling was done was replaced by the LOAEL or NOAEL. This was done to because there was no available tested software for performing BMD modeling in such a context and because of limitations in time and resources to develop such software. However, the relative degree of uncertainty/variability should be adequately captured in the use of the LOAEL or NOAEL. The graphical depiction of the HEC_{99} or HED_{99} using these alternative PODs is shown in the following files:

Appendix.linked.files\AppF.Non-cancer.HECs.AltPOD.Plots.rodent.inhalation.studies.TCE.DRAFT.pdf

Appendix.linked.files\AppF.Non-cancer.HECs.AltPOD.Plots.rodent.oral.studies.TCE.DRAFT.pdf

Appendix.linked.files\AppF.Non-cancer.HEDs.AltPOD.Plots.rodent.inhalation.studies.TCE.DRAFT.pdf

Appendix.linked.files\AppF.Non-cancer.HEDs.AltPOD.Plots.rodent.oral.studies.TCE.DRAFT.pdf

F.6. Summary of PODs for critical studies and effects supporting the RfC and RfD

This section summarizes the selection and/or derivation of PODs from the critical studies and effects that support the RfC and RfD. In particular, for each endpoint, the following are described: the dosimetry (adjustments of continuous exposure, PBPK dose metrics), selection of BMR and BMD model (if BMD modeling was performed), and derivation of the human equivalent concentration or dose for a sensitive individual (if PBPK modeling was used). The dose metric selection for different endpoints is discussed in Section 5.1.3.1.

F.6.1. NTP (1988) – BMD modeling of toxic nephropathy in rats

The critical endpoint here is toxic nephropathy in female Marshall rats (NTP, 1988), which was the most sensitive sex/strain in this study, although the differences among different sex/strain combinations was not large (BMDLs differed by ≤ 3-fold).

F.6.1.1. *Dosimetry and BMD modeling*

Rats were exposed to 500 or 1000 mg/kg/d, 5 d/wk, for 104 weeks. The primary dose metric was selected to be average amount of DCVC bioactivated/$kg^{3/4}$/d, with median estimates from the PBPK model for the female Marshall rats in this study of 0.47 and 1.1.

Figure F.10 shows BMD modeling for the dichotomous models used (see F.5.1, above). The log-logistic model with slope constrained to ≥ 1 was selected because (i) the log-logistic model with unconstrained slope yielded a slope estimate < 1 and (ii) it had the lowest AIC.

The iPOD of 0.0132 mg DCVC bioactivated/$kg^{3/4}$/d was a BMDL for a BMR of 5% extra risk. This BMR was selected because toxic nephropathy is a clear toxic effect. This BMR required substantial extrapolation below the observed responses (about 60%); however, the response level seemed warranted for this type of effect and the ratio of the BMD to the BMDL was not large (1.56 for the selected model).

F.6.1.2. *Derivation of HEC_{99} and HED_{99}*

The HEC99 and HED99 are the lower 99th percentiles for the continuous human exposure concentration and continuous human ingestion dose that lead to a human internal dose equal to the rodent iPOD. The derivation of the HEC_{99} of 0.0056 ppm and HED_{99} of 0.00338 mg/kg/d for the 99th percentile for uncertainty and variability are shown in Figure F.11. These values are used as this critical effect's POD to which additional UFs are applied.

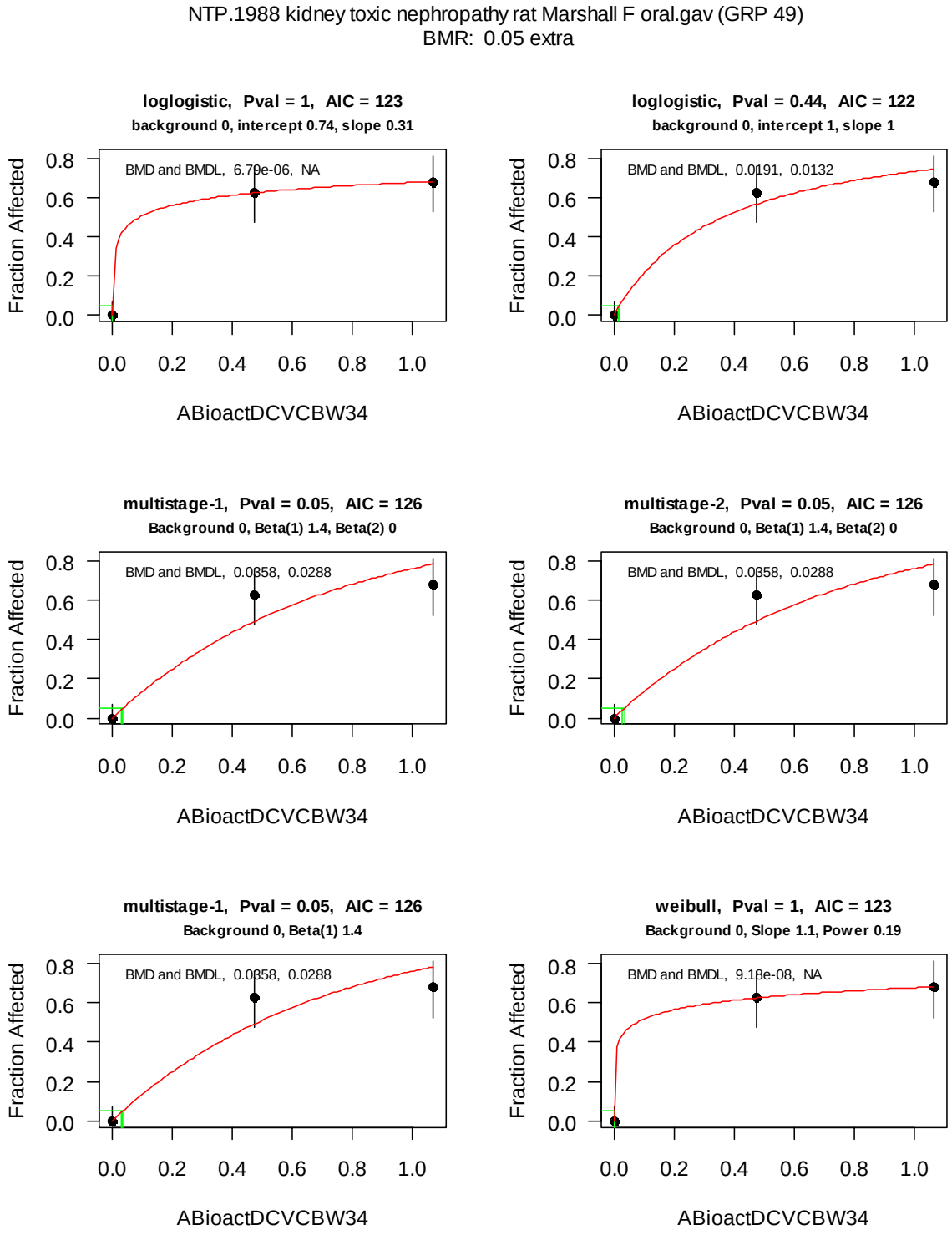

Figure F.10. BMD modeling of NTP (1988) toxic nephropathy in female Marshall rats.

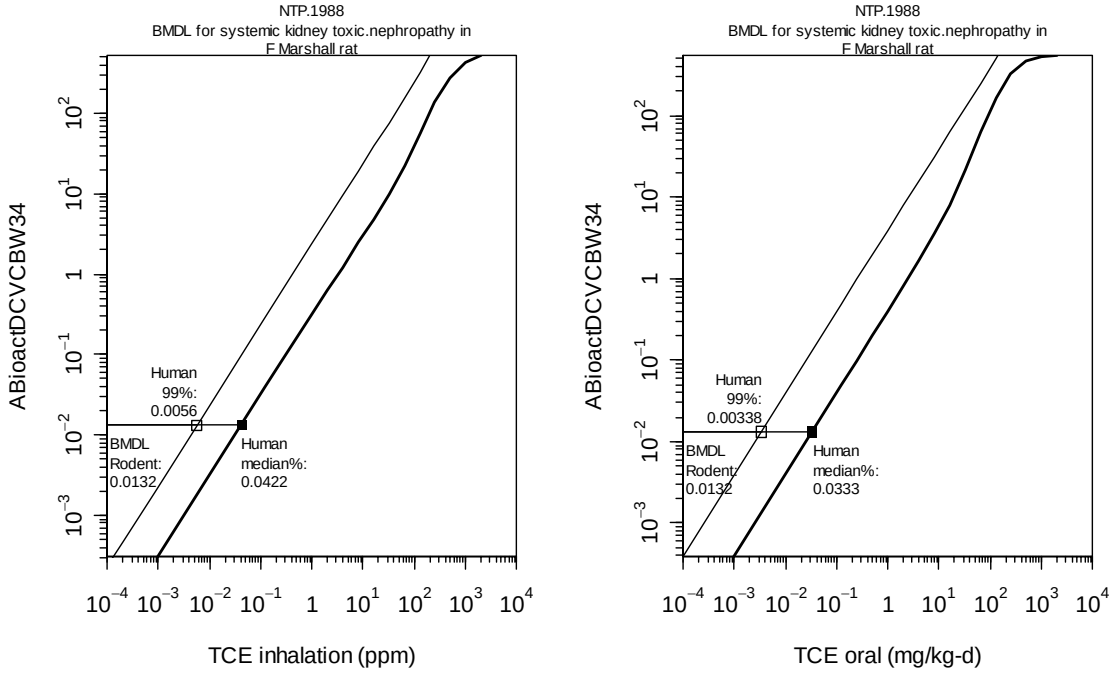

Figure F.11. Derivation of HEC99 and HED99 corresponding to the rodent iPOD from NTP (1988) toxic nephropathy in rats.

F.6.2. NCI (1976) – LOAEL for toxic nephrosis in mice

The critical endpoint here is toxic nephrosis in female B6C3F1 mice (NCI, 1976), which was the most sensitive sex in this study, although the LOAEL for males differed by less than 50%.

F.6.2.1. *Dosimetry*

Mice were exposed to a time-weighted average of 869 and 1739 mg/kg/d, 5 d/wk, for 78 weeks. BMD modeling was not performed because the response at the LOAEL was > 90%. The primary dose metric was selected to be average amount of TCE conjugated with GSH/$kg^{3/4}$/d. In this study, the lower dose group was exposed to two different dose levels (700 mg/kg/d for 12 weeks and 900 mg/kg/d for 66 weeks). The median estimates from the PBPK model for the two dose levels were 0.583 and 0.762 mg TCE conjugation with GSH/$kg^{3/4}$/d. Applying the same time-weighted averaging gives an iPOD LOAEL of 0.735 mg TCE conjugation with GSH/$kg^{3/4}$/d.

F.6.2.2. *Derivation of HEC_{99} and HED_{99}*

The HEC99 and HED99 are the lower 99th percentiles for the continuous human exposure concentration and continuous human ingestion dose that lead to a human internal dose equal to the rodent iPOD. The derivation of the HEC_{99} of 0.50 ppm and HED_{99} of 0.30 mg/kg/d for the 99th percentile for uncertainty and variability are shown in Figure F.12. These values are used as this critical effect's POD to which additional UFs are applied.

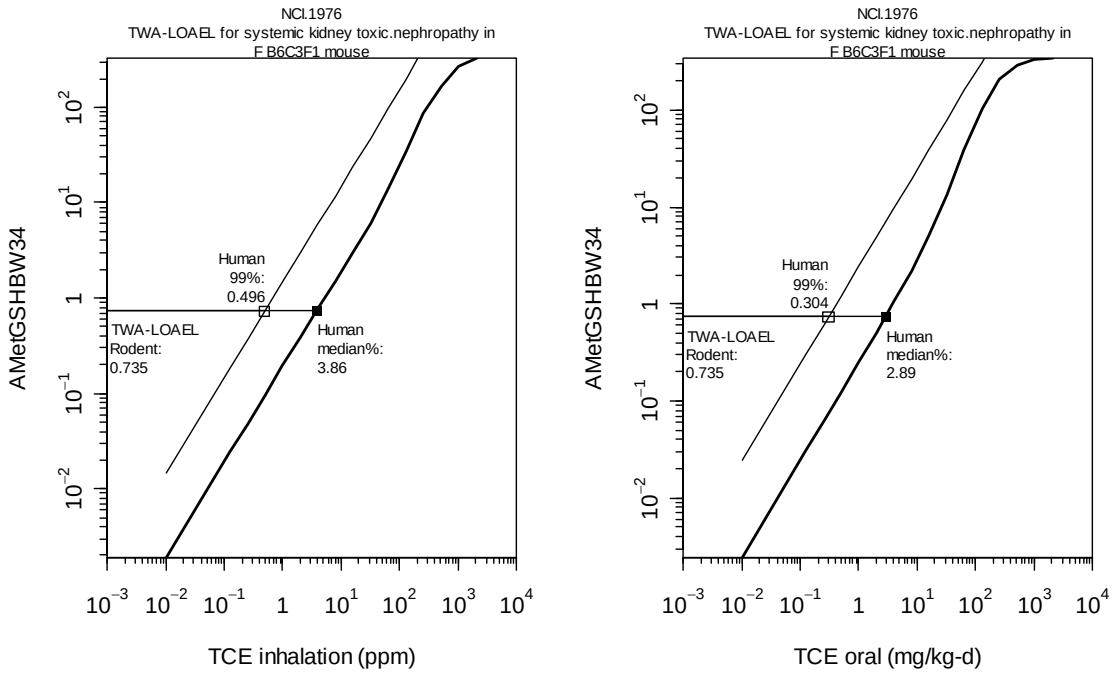

Figure F.12. Derivation of HEC99 and HED99 corresponding to the rodent iPOD from NTP (1988) toxic nephrosis in mice.

F.6.3. Woolhiser et al. (2006) – BMD modeling of increased kidney weight in rats

The critical endpoint here is increased kidney weights in female SD rats (Woolhiser et al., 2006).

F.6.3.1. *Dosimetry and BMD modeling*

Rats were exposed to 100, 300, and 1000, 6 hr/d, 5 d/wk, for 4 weeks. The primary dose metric was selected to be average amount of DCVC bioactivated/$kg^{3/4}$/d, with median estimates from the PBPK model for this study of 0.038, 0.10, and 0.51.

Figure F.13 shows BMD modeling for the continuous models used (see F.5.2, above). The Hill model with constant variance was selected because it had the lowest AIC and because other models with the same AIC either were a power model with power parameter <1 or had poor fits to the control dataset.

The iPOD of 0.0309 mg DCVC bioactivated/$kg^{3/4}$/d was a BMDL for a BMR of 10% weight change, which is the BMR typically used by EPA for body weight and organ weight changes. The response used in each case was the organ weight as a percentage of body weight, to account for any commensurate decreases in body weight, although the results did not differ much when absolute weights were used instead.

F.6.3.2. *Derivation of HEC_{99} and HED_{99}*

The HEC99 and HED99 are the lower 99th percentiles for the continuous human exposure concentration and continuous human ingestion dose that lead to a human internal dose equal to the rodent iPOD. The derivation of the HEC_{99} of 0.0131 ppm and HED_{99} of 0.00791 mg/kg/d for the 99th percentile for uncertainty and variability are shown in Figure F.14. These values are used as this critical effect's POD to which additional UFs are applied.

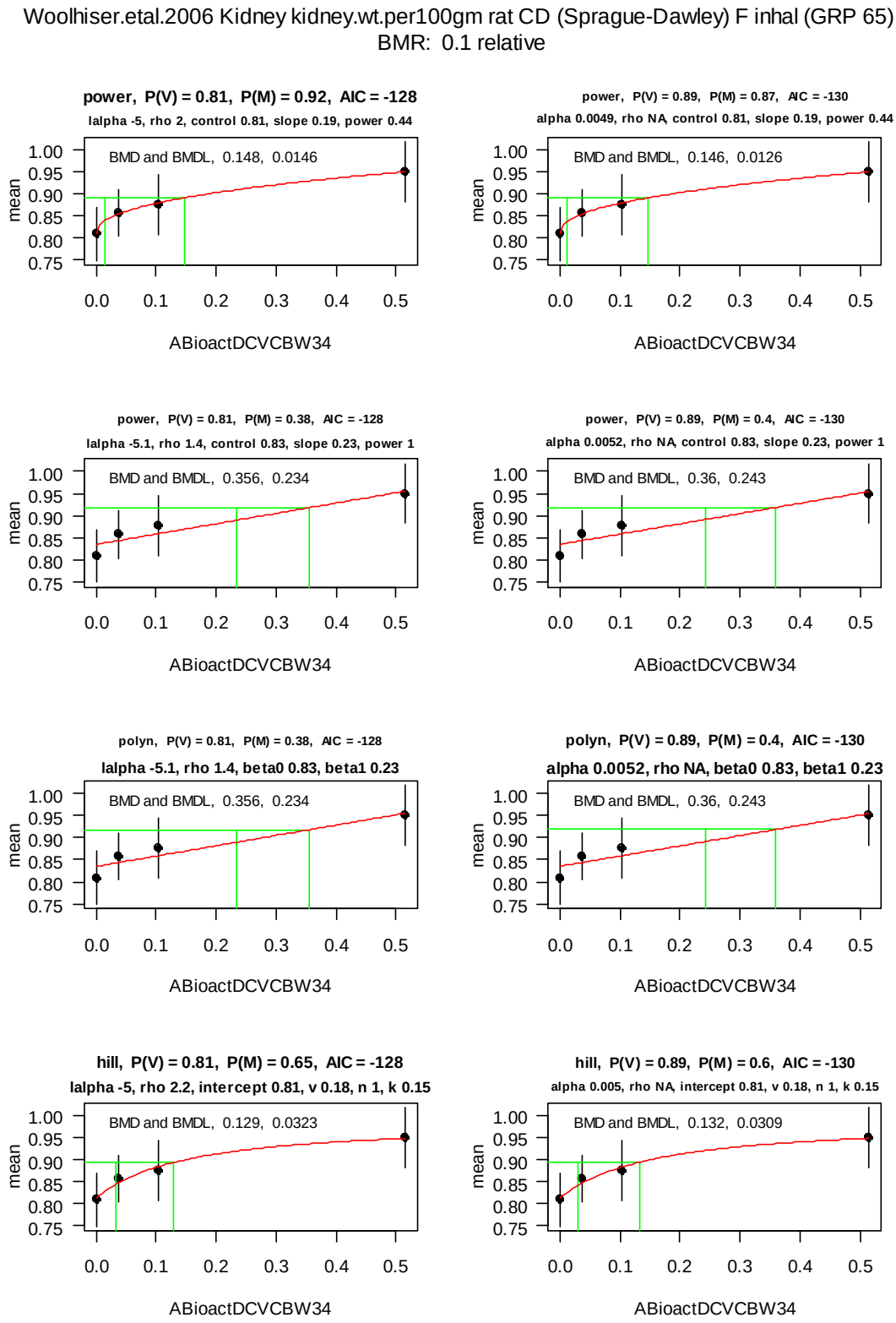

Figure F.13. BMD modeling of Woolhiser et al. (2006) for increased kidney weight in female SD rats.

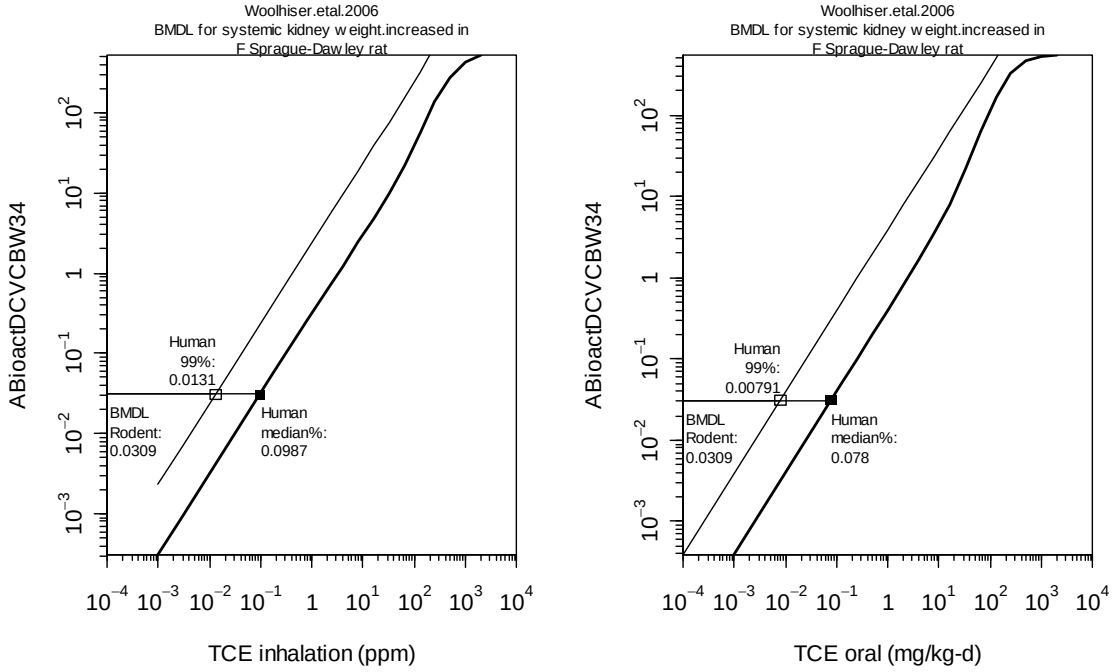

Figure F.14. Derivation of HEC99 and HED99 corresponding to the rodent iPOD from Woolhiser et al. (2006) for increased kidney weight in rats.

F.6.4. Keil et al. (2009) – LOAEL for decreased thymus weight and increased anti-dsDNA and anti-ssDNA antibodies in mice

The critical endpoints here are decreased thymus weight and increased anti-dsDNA and anti-ssDNA antibodies in female B6C3F1 mice (Keil et al., 2009).

F.6.4.1. *Dosimetry*

Mice were exposed to 1400 and 14000 ppb in drinking water, with an average dose estimated by the authors to be 0.35 and 3.5 mg/kg/d, for 30 weeks. The dose-response relationships were sufficiently supralinear that BMD modeling failed to produce an adequate fit. The primary dose metric was selected to be the average amount of TCE metabolized/$kg^{3/4}$/d. The lower dose group was the LOAEL for both effects, and the median estimate from the PBPK model at that exposure level was 0.139 mg TCE metabolized/$kg^{3/4}$/d, which is used as the rodent iPOD.

F.6.4.2. *Derivation of HEC_{99} and HED_{99}*

The HEC99 and HED99 are the lower 99th percentiles for the continuous human exposure concentration and continuous human ingestion dose that lead to a human internal dose equal to the rodent iPOD. The derivation of the HEC_{99} of 0.0332 ppm and HED_{99} of 0.0482 mg/kg/d for the 99th percentile for uncertainty and variability are shown in Figure F.15. These values are used as this critical effect's POD to which additional UFs are applied.

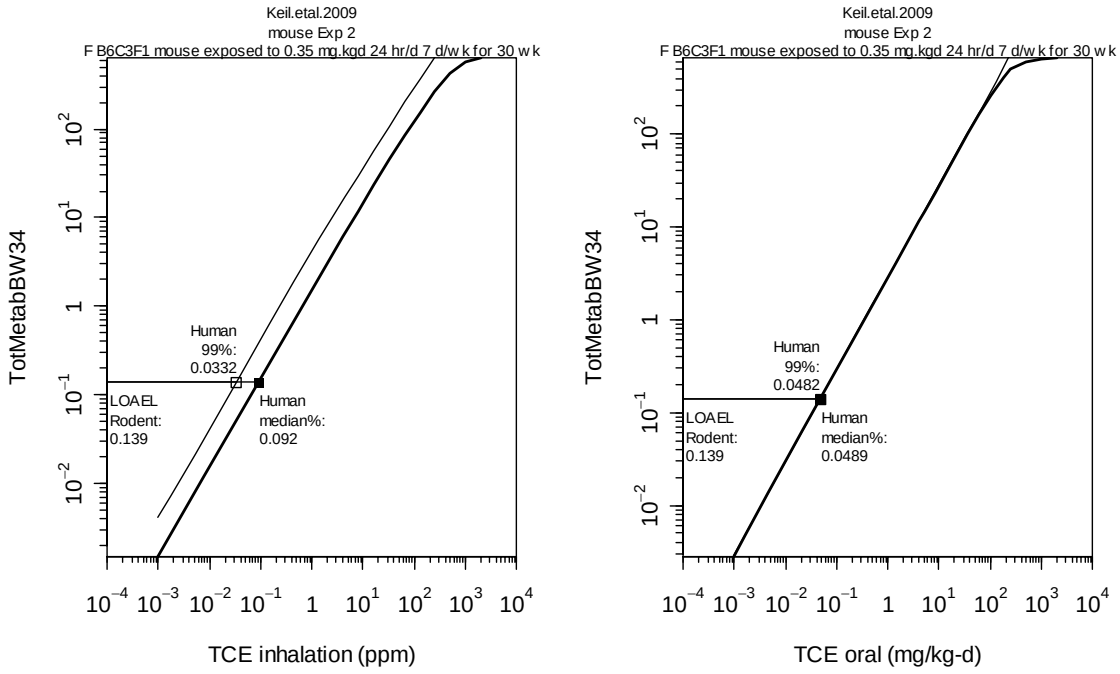

Figure F.15. Derivation of HEC99 and HED99 corresponding to the rodent iPOD from Keil et al. (2009) for decreased thymus weight and increased anti-dsDNA and anti-ssDNA antibodies in mice.

F.6.5. Johnson et al. (2003) – BMD modeling of fetal heart malformations in rats

The critical endpoint here is increased fetal heart malformations in female SD rats (Johnson et al., 2006).

F.6.5.1. *Dosimetry and BMD modeling*

Rats were exposed to 2.5 ppb, 250 ppb, 1.5 ppm, or 1,100 ppm TCE in drinking water for 22 days (GD122). The primary dose metric was selected to be average amount of TCE

metabolized by oxidation/kg$^{3/4}$/d, with median estimates from the PBPK model for this study of 0.00031, 0.033, 0.15, and 88.

As discussed previously in Section F.4.2.1, from results of nested loglogistic modeling of these data, with the highest dose group dropped, the iPOD of 0.0142 mg TCE metabolized by oxidation/kg$^{3/4}$/d was a BMDL for a BMR of 1% increased in incidence in pups. A 1% extra risk of a pup having a heart malformation was used as the BMR because of the severity of the effect; some of the types of malformations observed could have been fatal.

F.6.5.2. *Derivation of HEC_{99} and HED_{99}*

The HEC99 and HED99 are the lower 99th percentiles for the continuous human exposure concentration and continuous human ingestion dose that lead to a human internal dose equal to the rodent iPOD. The derivation of the HEC_{99} of 0.00365 ppm and HED_{99} of 0.00515 mg/kg/d for the 99th percentile for uncertainty and variability are shown in Figure F.16. These values are used as this critical effect's POD to which additional UFs are applied.

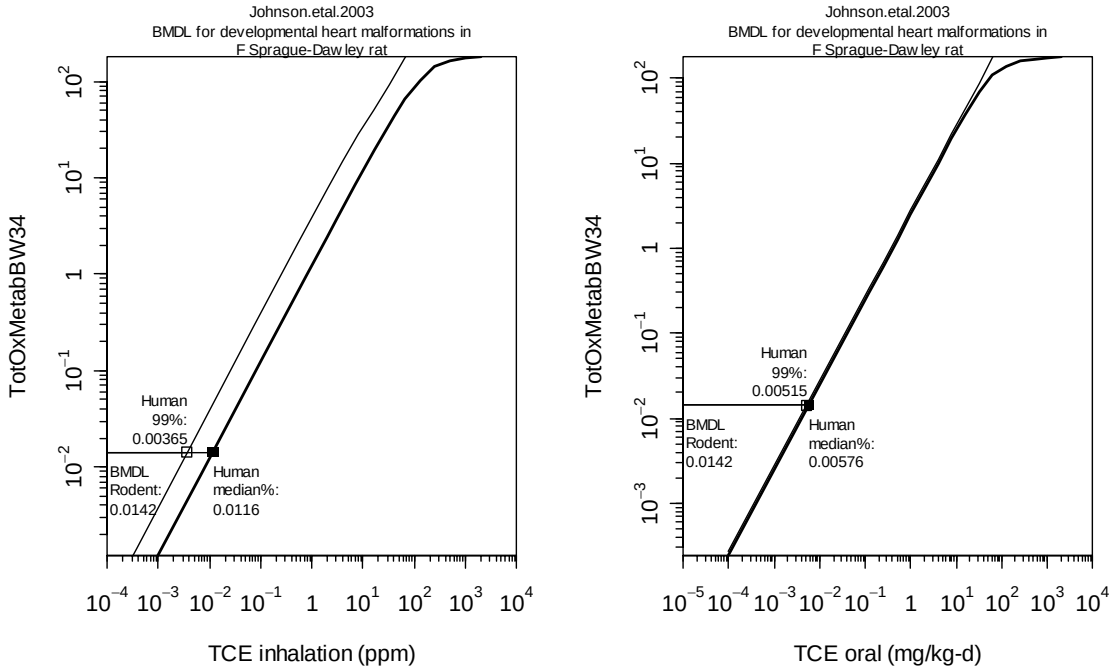

Figure F.16. Derivation of HEC99 and HED99 corresponding to the rodent iPOD from Johnson et al. (2003) for increased fetal cardiac malformations in female SD rats using the total oxidative metabolism dose metric.

F.6.6. Peden-Adams et al. (2006) – LOAEL for decreased PFC response and increased delayed-type hypersensitivity in mice

The critical endpoints here are decreased PFC response and increased delayed-type hypersensitivity in mice exposed pre- and post-natally (Peden-Adams et al., 2006).

Mice were exposed to 1400 and 14000 ppb in drinking water, with an average dose in the dams estimated by the authors to be 0.37 and 3.7 mg/kg/d, from GD0 to post-natal ages of 3 or 8 weeks. The dose-response relationships were sufficiently supralinear that BMD modeling failed to produce an adequate fit. In addition, because of the lack of an appropriate PBPK model and parameters to estimate internal doses given the complex exposure pattern (placental and lactational transfer, and pup ingestion post-weaning), no internal dose estimates were made. Therefore, the LOAEL of 0.37 mg/kg/d on the basis of applied dose was used as the critical effect's POD to which additional UFs are applied.

F.7. References

Box GEP, Hunter WG, Hunter JS. (1978). Statistics for Experimenters, New York: John Wiley & Sons.

Buben, JA; O'Flaherty, EJ. (1985) Delineation of the role of metabolism in the hepatotoxicity of trichloroethylene and perchloroethylene: a dose-effect study. Toxicol Appl Pharmacol 78:105-122.

Carney, EW; Thorsrud, BA; Dugard, PH; Zablotny, CL. (2006) Developmental toxicity studies in Crl:Cd (SD) rats following inhalation exposure to trichloroethylene and perchloroethylene. Birth Defects Research (Part B) 77:405-412.

Chia SE, Ong CN, Tsakok MF, Ho A. (1996) Semen parameters in workers exposed to trichloroethylene. Reprod Toxicol 10(4):295-299.

Crofton, KM; Zhao, X. (1997) The ototoxicity of trichloroethylene: extrapolation and relevance of high-concentration, short-duration animal exposure data. Fundam Appl Toxicol 38(1):101–106.

Filipsson, A.F., K. Victorin. (2003). Comparison of available benchmark dose softwares and models using trichloroethylene as a model substance. Regulatory Toxicology and Pharmacology 37:343-355

George, JD; Reel, JR; Myers, CB; Lawton, AD; Lamb, JC. (1986) Trichloroethylene: reproduction and fertility assessment in F344 rats when administered in the feed. RTI Project No. 310-2344, NTP-86-085. National Institute of Environmental Health Sciences, National Toxicology Program, RTP, NC.

Griffin JM, Gilbert KM, Lamps LW, Pumford NR. 2000b. CD4(+) T-cell activation and induction of autoimmune hepatitis following trichloroethylene treatment in MRL+/+ mice. Toxicol Sci 57:345-352.

Johnson, PD; Goldberg, SJ; Mays, MZ; Dawson, BV. (2003) Threshold of trichloroethylene contamination in maternal drinking waters affecting fetal heart development in the rat. Environ Health Perspect 111(3):289-292.

Keil, DE; Peden-Adams, MM; Wallace, S; Ruiz, P; Gilkeson, GS. (2009) Assessment of trichloroethylene (TCE) exposure in murine strains genetically-prone and non-prone to develop autoimmune disease. Journal of Environmental Science and Health, Part A 44: 443-453.

Kjellstrand P, Holmquist B, Alm P, Kanje M, Romare S, Jonsson I, Månsson L, Bjerkemo M. (1983a) Trichloroethylene: further studies of the effects on body and organ weights and plasma butyrylcholinesterase activity in mice. Acta Pharmacol Toxicol (Copenh) 53(5):375-84.

Kjellstrand P, Holmquist B, Mandahl N, Bjerkemo M. (1983b) Effects of continuous trichloroethylene inhalation on different strains of mice. Acta Pharmacol Toxicol (Copenh) 53(5):369-74.

Land, PC; Owen, EL; Linde, HW. (1981) Morphologic changes in mouse spermatozoa after exposure to inhalational anesthetics during early spermatogenesis. Anesthesiology 54:53-56.

Maltoni, C; Lefemine, G; Cotti, G. (1986) Experimental research on trichloroethylene carcinogenesis. In: Maltoni, C; Mehlman MA., eds. Vol. 5. Archives of research on industrial carcinogenesis. Princeton, NJ: Princeton Scientific Publishing;

Mhiri, C; Choyakh, F; Ben, HM; et al. (2004) Trigeminal somatosensory evoked potentials in trichloroethylene-exposed workers. Neurosciences 9(2):102–107.

Moser, Cheek & MacPhail. A multidisciplinary approach to toxicological screening III. Neurotbehavioral toxicity. J Toxicol. Environ. Hlth., 1995, 45, 173-210.

Narotsky, MG; Weller, EA; Chinchilli, VM; Kavlock, RJ. (1995) Nonadditive developmental toxicity in mixtures of trichloroethylene, di(2-ethylhexyl) phthalate, and heptachlor in a 5 x 5 x 5 design. Fundam Appl Toxicol 27:203-216.

NCI (National Cancer Institute). (1976) Carcinogenesis bioassay of trichloroethylene. Division of Cancer Cause and Prevention, National Cancer Institute, U.S. Department of Health, Education, and Welfare, DHEW Publication No. (NIH) 76-802, Technical Report Series No. 2, 218 pages; NCI-CG-TR-2; NTIS PB254122. http://ntp.niehs.nih.gov/ntp/htdocs/LT_rpts/tr002.pdf.

NTP (National Toxicology Program). (1988) Toxicology and carcinogenesis studies of trichloroethylene (CAS no. 79-01-6) in four strains of rats (ACI, August, Marshall, Osborne-Mendel) (gavage studies). Public Health Service, U.S. Department of Health and Human Services; NTP TR-273; NIH Publication No. 88-2529. Available from the National Institute of Environmental Health Sciences, Research Triangle Park, NC, and the National Technical Information Service, Springfield, VA; PB88-218896. http://ntp.niehs.nih.gov/ntp/htdocs/LT_rpts/tr273.pdf.

NTP (National Toxicology Program). (1990) Carcinogenesis Studies of Trichloroethylene (Without Epichlorhydrin) (CAS No. 79-01-6) in F344/N Rats and B6C3F1 Mice (Gavage Study). NTP TR 243. Research Triangle Park, NC: U.S Department of Health and Human Services.

Peden-Adams MM, Eudaly JG, Heesemann LM, Smythe J, Miller J, Gilkeson GS, et al. (2006). Developmental immunotoxicity of trichloroethylene (TCE): studies in B6C3F1 mice. J Environ Sci Health A Tox Hazard Subst Environ Eng 41:249-271.

Snedecor GW, Cochran WG. (1980). Statistical Methods (7th ed.), Ch. 9.12 and Ch 9.14 (pp.169-172)

U.S. EPA (Environmental Protection Agency) (2008b). Benchmark Dose Technical Guidance (Inter-Agency Review Draft).

U.S. EPA (Environmental Protection Agency). (1994) Methods for derivation of inhalation reference concentrations and application of inhalation dosimetry. Environmental Criteria and Assessment Office, Office of Health and Environmental Assessment, Washington,

Washington, DC; EPA/600/8-90/066F. Available from: National Technical Information Service, Springfield, VA; PB2000-500023.

Woolhiser, MR; Krieger, SM; Thomas, J; Hotchkiss, JA. (2006) Trichloroethylene (TCE): Immunotoxicity potential in CD rats following a 4-week vapor inhalation exposure. Dow Chemical Company, Toxicology & Environmental Research and Consulting, Midland, MI, Study ID 031020, July 5, 2006, unpublished.